Properties of WE43 Metal Matrix Composites Reinforced with SiC Particles

B. Dybowski, T. Rzychoń, B. Chmiela and A. Gryc

Abstract It is well known that the properties of metal matrix composites depend upon the properties of the reinforcement phase, on the matrix and on the interface. A strong interface bonding without any degradation of the reinforcing phase is one of the prime objectives in the development of metal matrix composites. The objective of this work is to characterize the interface structure of WE43/SiC particles composite and their mechanical properties at ambient and elevated temperatures. Magnesium alloys containing yttrium and neodymium are known to have high specific strength, good creep and corrosion resistance up to 523 K. The addition of SiC ceramic particles strengthens the metal matrix composite resulting in better wear and creep resistance while maintaining good machinability. In the present study, WE43 magnesium matrix composite reinforced with SiC particulates was fabricated by stir casting. The SiC particles with 15, 45 and 250 μm diameter were added to the WE43 alloy. Microstructure characterization of WE43 MMC with 45 μm showed a relatively uniform reinforcement distribution and presence of inconsiderable porosity. Moreover, the Zr-rich particles at the particle/matrix interface were visible. The presence of SiC particles assisted in improving hardness and decreasing the tensile strength creep resistance.

Keywords WE43 MMC · Stir casting · Mechanical properties · Creep resistance · Sic reinforcement

B. Dybowski · T. Rzychoń (✉) · B. Chmiela · A. Gryc
Faculty of Material Science and Metallurgy, Silesian University of Technology, Krasińskiego Street 8, 40-019 Katowice, Poland
e-mail: tomasz.rzychon@polsl.pl

B. Dybowski
e-mail: bartlomiej.dybowski@polsl.pl

B. Chmiela
e-mail: bartosz.chmiela@polsl.pl

A. Gryc
e-mail: gryadam@wp.pl

A. Öchsner and H. Altenbach (eds.), *Properties and Characterization of Modern Materials*, Advanced Structured Materials 33,
DOI 10.1007/978-981-10-1602-8_18

1 Introduction

Magnesium alloys are a more and more widely applied material in automotive and aerospace industries. The combination of low density (≈1.8 g/cm^3) and good mechanical properties of aluminium containing magnesium alloys (AZ, AM types) led to the application of these materials in structural elements operating at ambient temperature in the automotive and aerospace industries [1–4]. The very low maximal working temperature of these alloys (about 120 °C) stopped the further application of these in elements of, for example, engine blocks. The addition of rare earth elements (RE) to the aluminium containing alloys or even replacing aluminium with them, causes formation of thermally stable Al-RE or Mg-RE phases, thus increasing operation temperature up to 250 °C [5, 6].

Further increases in creep resistance of magnesium alloys may be achieved by an introduction of ceramic particles to the alloy structure. It has been revealed that the addition of 3 % of nanoscaled SiC particles to pure magnesium increases its creep resistance to the level of commercial Mg-RE alloys [7]. The majority of authors produce magnesium MMC reinforced with ceramic particles by means of milling and sintering [8–11]. This method, however, is difficult to apply in commercial production, mainly because of the difficulties in the production of more complicated elements. For this reason, stir casting seems to be an effective method to manufacture more complex structures [10]. The main drawback of this method is, the tendency of the particles to cluster. This leads to the formation of agglomerates, dramatically decreasing mechanical properties of the material [12]. To avoid agglomeration of the particles, a relatively long time of stirring at elevated temperature is needed, which in turn, may result in degradation of the ceramic particles. A too short stirring time, or stirring at too low a temperature may in turn lead to a not uniformly distributed reinforcing phase.

The following paper presents results of the investigations on the mechanical properties at ambient and elevated temperature of the stir cast WE43 MMC reinforced with SiC particulates.

2 Research Material and Methodology

The material used in this research was the WE43 metal matrix composite (MMC) reinforced with SiC particulates. The composite has been reinforced with particulates with mean diameter d = 15, 45 μm as well as 200 μm. The volume fraction of the reinforcement was equal to 10 %. Additionally, composites with reinforced with the 0 ÷ 6 % of 45 μm particulates were investigated. All composites were produced by means of stir casting. Commercial ingots of WE43 magnesium alloy were melted in a resistance furnace under the protective atmosphere of 99.999 % Ar. The melt was homogenised for about 20 min. at 720 and

780 °C. The Mg–Y, Mg–Zr and Mg–Nd hardeners were added to compensate the alloy's chemical composition. Particulates preheated up to 300 °C were added to the liquid alloy after the homogenisation. The suspension was then stirred for about 15 min. Immediately after the stirring process, the composite was poured into the graphite moulds, preheated up to 200 °C. The pouring process as well as composite solidification were also conducted under the Ar protective atmosphere. The researches were done on specimens in both as-cast as age hardened specimens. Solution treatment of the composites was conducted at 525 °C for 8 h, while aging at 250 °C for 16 h.

The microstructure observations of the composites were done on microsections prepared with the following procedure: cutting, grinding on the SiC abrasive papers with grades 120 ÷ 2400, polishing on the diamond suspensions with the mean grain size 6, 3 and 1 μm and final polishing on Struers OP-AN alumina suspension with a grain size 0.05 μm. The microstructure of the composite was investigated on un-etched specimens. Observations were done on an Olympus GX71 light microscope (LM) as well as a Hitachi S3400N scanning electron microscope (SEM). The investigations were also conducted by means of scanning-transmission electron microscopy (STEM) on a Hitachi HD2300A STEM. Specimens for the STEM investigations were prepared with a FIB 2100 focused ion beam microscope. Chemical composition of the phases was analysed by energy dispersive X-Ray spectroscopy (EDS).

Phase analysis were done by X-Ray diffraction (XRD) on a JEOL JDX-7S diffractometer with a copper anode. Registration of XRD patterns was performed by 0.02° stepwise regression for 2θ ranging from 10° to 90° 2θ. Phase identification was performed using the ICDD PDF-4+database.

The mechanical properties and the creep resistance of the composites were investigated on a Kappa 50DS tensile testing machine. Creep tests were conducted at 250 °C with a load of 90 MPa. The testing time was equal to 120 h. HV2 Vickers hardness was investigated on a Duramin A300 hardness tester.

3 Research Results

3.1 Composite Microstructure in the as Cast Condition

The microstructure of the composite's matrix in the as-cast state consists of α-Mg dendrites and the eutectic equilibrium β-Mg_5RE phase [5]. The eutectic phase is distributed homogenously within the interdendritic regions (Fig. 1a). Sporadically, Y-and Zr- enriched non-metallic inclusions are observed in the WE43 matrix microstructure (Fig. 1b). Composites prepared with 45 μm particulates are characterized by a relatively homogenous distribution of the reinforcing phase (Fig. 2a). Composites reinforced with 15 μm particles also show a homogenous microstructure, however, only if stirred at 780 °C. After stirring at 720 °C such small particles

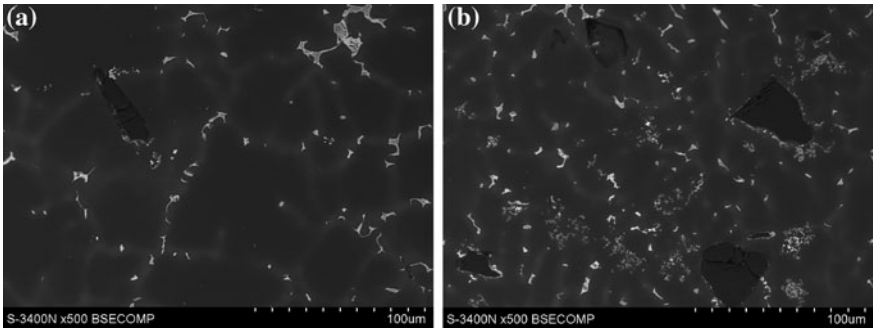

Fig. 1 Microstructure of the WE43 MMC reinforced with SiC particulates, SEM

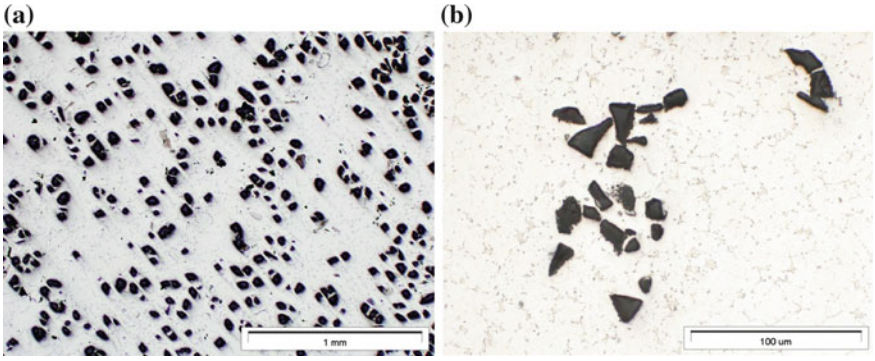

Fig. 2 Reinforcement in the WE43 MMC, LM; **a** composite reinforced with 45 μm SiC particulates; **b** composite reinforced with 15 μm SiC particulates, stirred at 720 °C

tend to form agglomerates (Fig. 2b). Composites reinforced with 250 μm SiC particles exhibit homogenous distribution at the transverse section of the research cast. However, such big particles settle down both in the crucible and mould, forming an inhomogeneous distribution of the reinforcement at the longitudinal section of the cast.

The stirring of the melt at 780 °C leads to reactions between the reinforcement and liquid alloy. Massive YSi particles are formed at the SiC/matrix interface. Degradation of the SiC particles led to the dissolution of silicon within the alloy and formation of Mg_2Si phase within the composite matrix (Fig. 3a). Stirring and pouring of the composite at the 720 °C led to much smaller reactions between the liquid alloy and reinforcement. The SiC particles are covered with a thin, Zr enriched layer, consisting of fine Zr–Si (mainly Zr_2Si) and Y_2O_3 particles (Fig. 3b). The more detailed investigations on the composite microstructure will be published elsewhere.

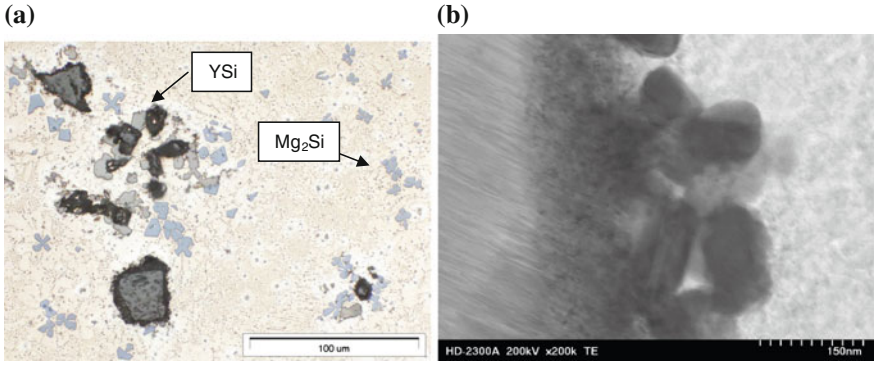

Fig. 3 Interfaces between SiC particulates and WE43 matrix; **a** composite stirred at 780 °C, LM; **b** composite stirred at 720 °C, STEM

3.2 Composite Microstructure After the Heat Treatment

The solution treatment of the composites at 525 °C led to the complete dissolution of eutectic β Mg_5RE phase within the α-Mg dendrites (Fig. 4). In the composites stirred at 720 °C further reactions between the alloy and SiC have not been observed. It indicates that the fine Zr–Si layer effectively hinders alloying elements to diffuse at an elevated temperature.

Aging of the composite stirred at 780 °C did not lead to precipitation of reinforcing phase. Yttrium bonded in the YSi phases cannot take a part in age-hardening process, thus leading to a lack of composite age-hardening response.

Aging of the composites stirred at 720 °C led to the precipitation of strengthening phases. Aging at 250 °C for 16 h leads to the precipitation of both β" with a $D0_{19}$ crystal structure and β' with orthorhombic crystal structure phases [13, 14]. These phases possess platelet-like morphology with a width of about 7–15 nm and lengths between 30 and 200 nm as well as a globular morphology with a diameter between 15 and 45 nm [15].

3.3 Mechanical Properties of the Composites in Ambient Temperature

The mechanical properties of the WE43 MMC reinforced with SiC particles in the as-cast state are shown in Table 1. Addition of SiC particulates significantly reduces the tensile strength of the WE43 alloy. It decreases both with the increasing size of the SiC particulates and their volume fraction. Yield strength and elongation of the composite also decrease after the addition of SiC particulates; however it

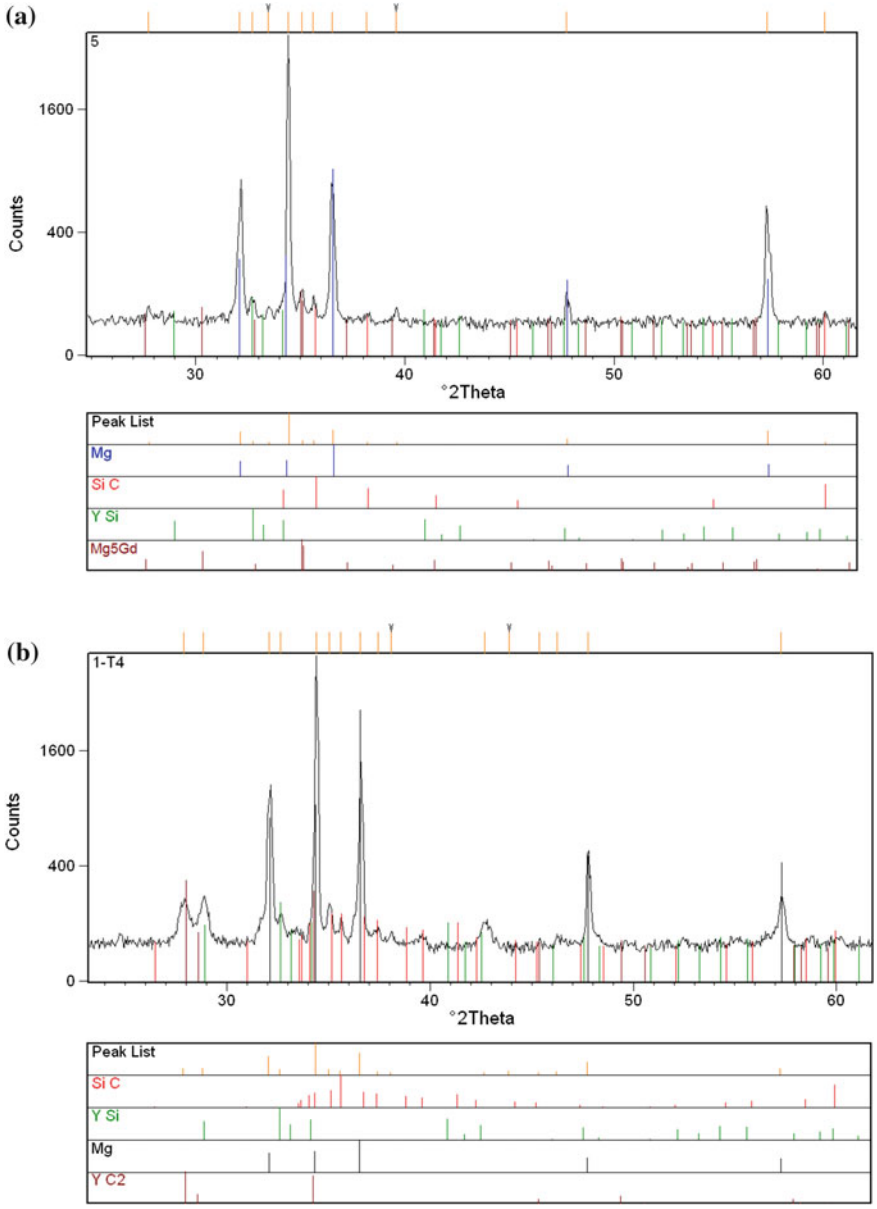

Fig. 4 XRD analysis results for the composite stirred at 780 °C; **a** composite in the as-cast condition; **b** composite after solution treatment at 525 °C

does not exhibit a further decrease with increasing volume fraction of the reinforcement. Hardness of the composites increases with increasing volume fraction and mean diameter of SiC particles.

Table 1 Mechanical properties of the WE43 MMC reinforced with SiC particulates in the as-cast condition

Material	Particle diameter (μm)	Stirring temperature (°C)	Stirring time (min)	Hardness HV2	R_m (MPa)	$R_{0,2}$ (MPa)	A_5 (%)
WE43	–	–	–	59 ± 4	166 ± 18	113 ± 9	6.7 ± 1.5
WE43 + 10 % SiC	15	720	15	68 ± 5	142 ± 4	103 ± 6	2.9 ± 0.3
WE43 + 10 % SiC	15	780	15	66 ± 7	146 ± 9	111 ± 12	2.8 ± 0.2
WE43 + 0.3 % SiC	45	720	15	61 ± 5	150 ± 1	112 ± 10	2.2 ± 1.3
WE43 + 2 % SiC	45	720	15	64 ± 7	151 ± 13	116 ± 6	2.2 ± 1.3
WE43 + 5 % SiC	45	720	15	68 ± 5	146 ± 7	110 ± 6	1.3 ± 0.4
WE43 + 10 % SiC	45	720	15	71 ± 6	149 ± 16	125 ± 14	3.0 ± 0.1
WE43 + 10 % SiC	250	720	15	81 ± 4	112 ± 11	89 ± 6	1.1 ± 0.1

Table 2 Mechanical properties of the WE43 MMC reinforced with 45 μm SiC particulates after the heat treatment

Material	Particle diameter (μm)	Stirring temperature (° C)	UTS (MPa)	YTS (MPa)	El. (%)
WE43 unreinforced	–	–	222 ± 4	153 ± 6	7.7 ± 1.3
WE43 + 0.3 % SiC	45	720	198 ± 10	147 ± 3	4.0 ± 2.0
WE43 + 2 % SiC	45	720	181 ± 20	146 ± 6	2.0 ± 1.5
WE43 + 5 % SiC	45	720	173 ± 16	148 ± 6	1.9 ± 1.3
WE43 + 10 % SiC	45	720	142 ± 24	115 ± 2	1.4 ± 2.2

Heat treatment of composites stirred at 720 °C causes a significant increase of their mechanical and plastic properties (Table 2), however, they are still lower than those exhibited by an unreinforced alloy. The beneficial effect of heat treatment is hindered by the increase of the reinforcement volume fraction. In the case of composites reinforced with 10 % of SiC particulates, the properties are the same as in the as-cast state.

Typical fracture surfaces of heat-treated, unreinforced SiC alloys are shown in Fig. 5. The fracture has a mixed character, with brittle and ductile regions recognizable. Numerous cleavage steps and facets suggest hindered propagation of the fracture. Many secondary cracks are observed at its surface. Fractures of the reinforced alloy are rich in SiC particles (Fig. 6a). Many secondary cracks nucleate at the SiC particles or at the interface between the particle and WE43 alloy. These cracks then propagate within the matrix (Fig. 6b).

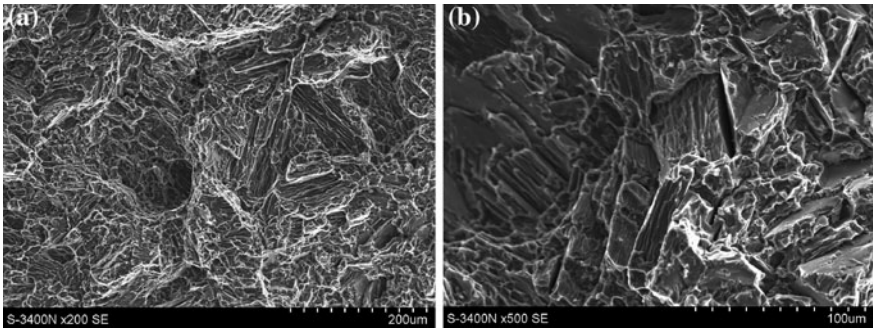

Fig. 5 Fracture surface in the unreinforced WE43 alloy after the tensile tests in the ambient temperature, SEM

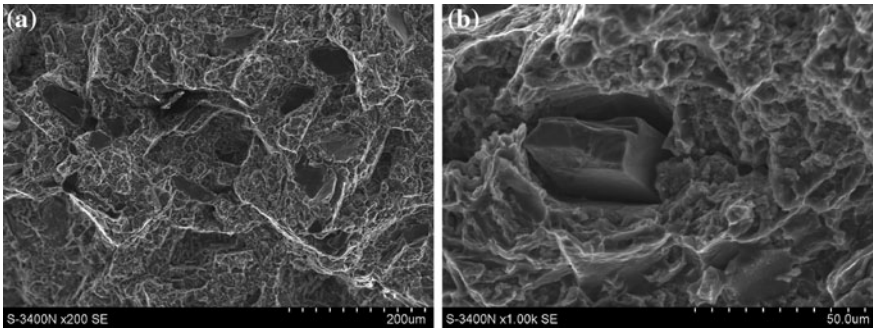

Fig. 6 Fracture surface in the SiC reinforced WE43 alloy after the tensile tests in the ambient temperature, SEM

3.4 Creep Resistance of the Composites

The creep tests were conducted on the heat treated composites reinforced with 45 μm SiC particulates at a temperature of 250 °C and at an applied stress of 90 MPa. The 120 h creep curves for some MMC WE43 are shown in Fig. 7. From the gradient of the secondary stage in the creep curves, the steady-state creep rate can be calculated and the results are shown in Table 3. Creep rate in the investigated composites increases with an increasing volume fraction of the SiC particulates. Creep strain at the rupture of the composites varies from 2.0 % up to 9.0 %, and does not exhibit any tendency with increasing volume fraction of the

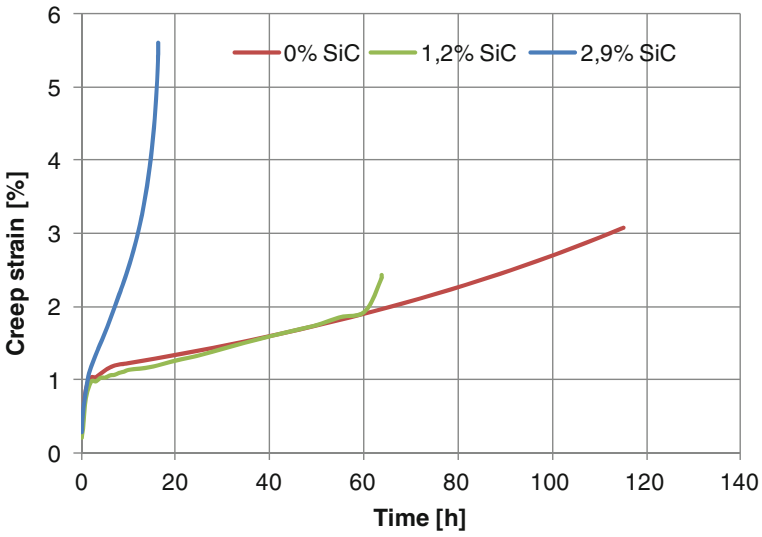

Fig. 7 Exemplary creep curves for the unreinforced and SiC reinforced WE43 alloy

Table 3 Creep properties of the WE43 MMC reinforced with 45 μm SiC particulates after the heat treatment

SiC volume fraction (%)	Rupture time (h)	Creep strain (%)	Creep rate $\dot{\varepsilon}$ (1/s)
0	–	3.2	4.13×10^{-8}
0.2	110	9.0	7.25×10^{-8}
1.2	66	2.4	4.42×10^{-8}
1.4	62	2.0	1.75×10^{-8}
2.0	37	2.4	1.23×10^{-7}
2.9	18.2	5.6	4.59×10^{-7}
3.5	14.3	5.7	6.12×10^{-7}
4.0	11	4.6	6.18×10^{-7}
5.6	6.6	3.3	7.47×10^{-7}
6.2	4.8	3.5	1.92×10^{-6}
6.3	8.5	3.4	6.35×10^{-7}
6.4	2.9	2.3	1.58×10^{-6}

reinforcement. It may be stated that, in majority it is similar to this, exhibited by an unreinforced WE43 alloy (3.2 %). The time to the rupture decreases with an increasing volume fraction of the SiC particulates (Fig. 8).

There are several creep mechanisms occurring within the composite matrix. First of all, strengthening fine β" and β' phases present in the heat treated alloy, undergo further transformations. Mengucci et al. [15] reports that precipitates in the WE43 alloy after heat treatment for 16 h at 250 °C are not bigger than 200 nm. The microstructure of the WE43 matrix alloy after the creep tests consist of much more coarse, precipitates of β phase (Fig. 9a) easily recognizable even with SEM microscopy (Fig. 9b). The length of these precipitates is usually higher than

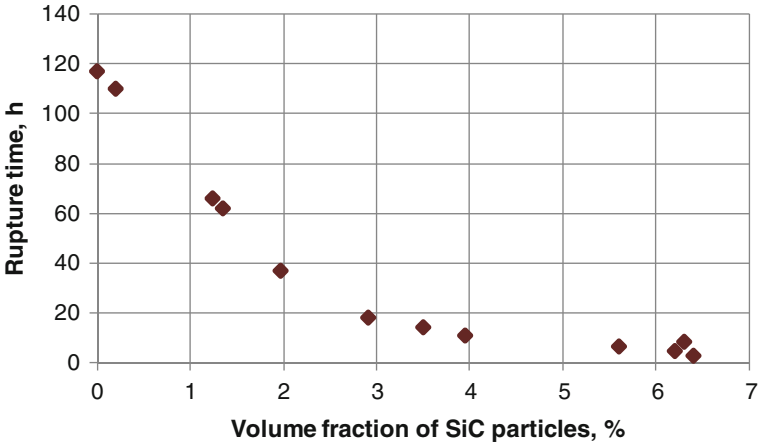

Fig. 8 Time to the rupture versus reinforcement volume fraction

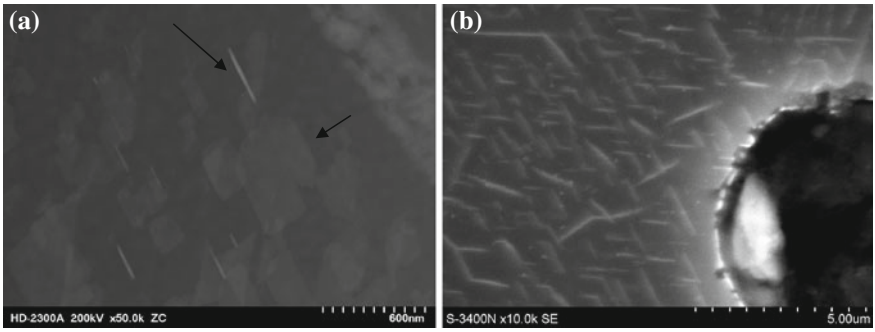

Fig. 9 Strengthening phases in the WE43 matrix alloy after creep tests

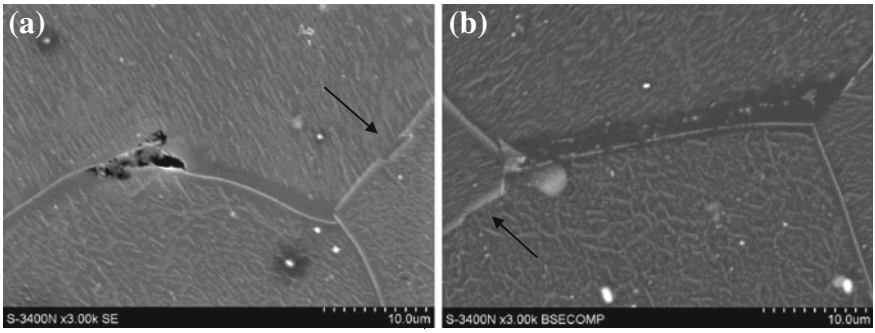

Fig. 10 Grain boundaries migration and zones depleted in the solute elements, SEM

300 nm and their width is equal to about 200 nm. The biggest precipitates observed by SEM are even a few micrometers long.

Temperature activated diffusion leads to the migration of grain boundaries in the direction of the applied load. The migration effects in the formation of solute element depleted zones in the vicinity of the boundaries (Fig. 10). It can be seen, that these denuded zones are clearly the weakest point in the microstructure, as many cracks nucleate within them (Fig. 11). The grain boundary sliding can be blocked by fine primary phase particles present within the structure (Fig. 12).

The creep cavities found within the composites microstructure are observed at the grain boundaries triple junctions. Nearly perfectly circular cavities are also observed within the WE43 magnesium alloy dendrites (Fig. 13). All above mentioned phenomena were observed both in unreinforced WE43 alloy as well as in the SiC reinforced composites.

No further transformations are observed at the interfaces between SiC particulates and the composite's matrix. The thin layer enriched in Zr and Si is still present, without significant thickening (Fig. 14a). At the layer, fine Zr–Si and Y_2O_3 (Fig. 15) phases are observed. A thin zone depleted in alloying elements is visible

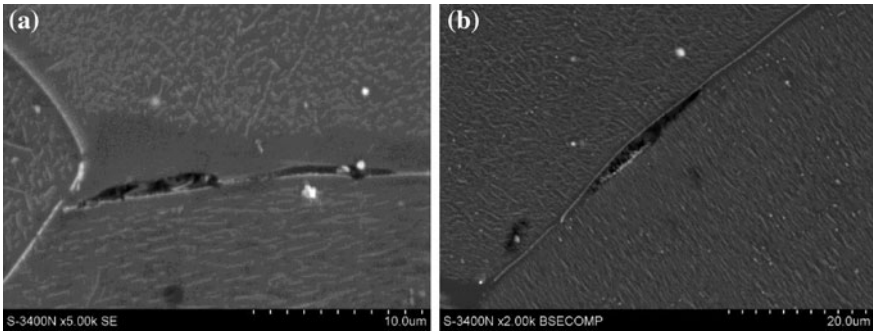

Fig. 11 Cracks in denuded zones at the grain boundaries, SEM

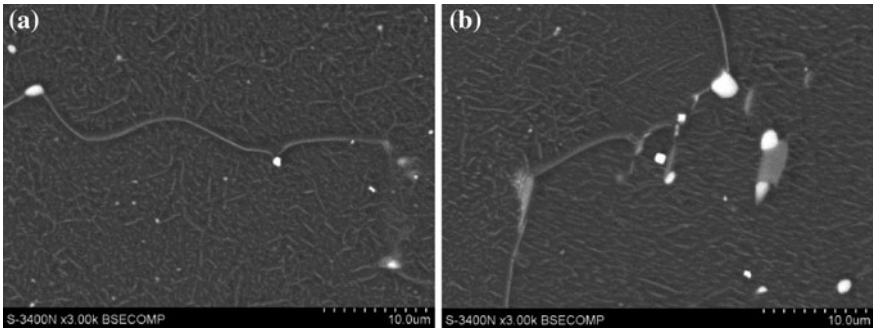

Fig. 12 Phases blocking grain boundaries sliding, SEM

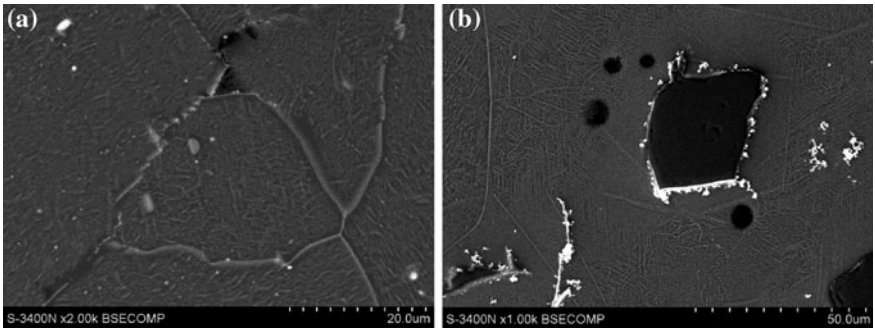

Fig. 13 Creep cavities in the WE43 alloy microstructure, SEM; **a** at the grain boundaries triple junctions; **b** within the α-Mg dendrites

near the particles (Fig. 14b). Even though the SiC/WE43 matrix interface did not undergo any transformations during the creep, many cracks are observed at the interfaces perpendicular to the applied loads (Fig. 16).

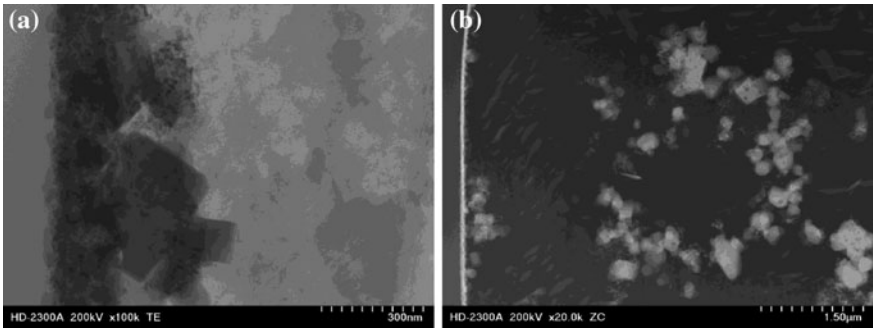

Fig. 14 SiC/WE43 interface, STEM; **a** Zr–Si layer and and Y_2O_3 phase; **b** Yttrium depleted zone between the particle and matrix

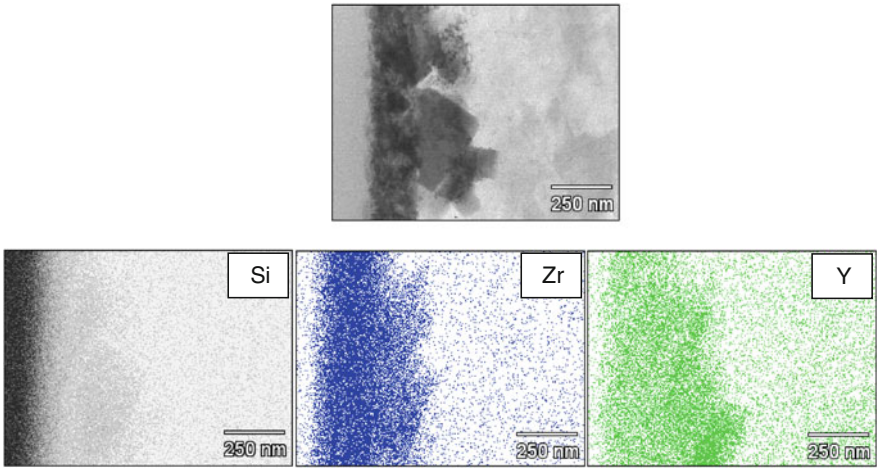

Fig. 15 Mapping of elements at the SiC/WE 43 matrix interface after the creep tests

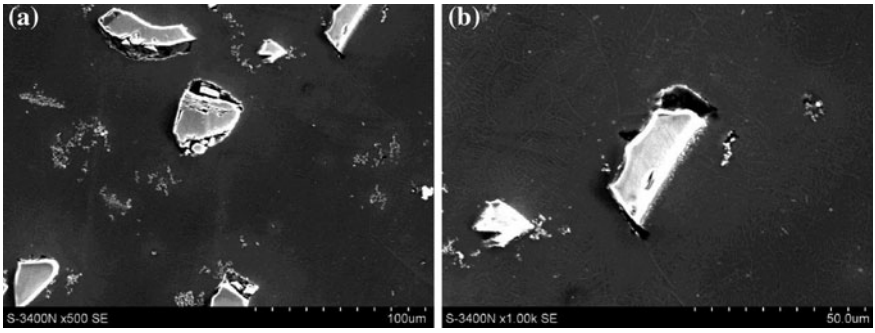

Fig. 16 Cracks at the SiC/WE43 interfaces perpendicular to the applied loads, SEM

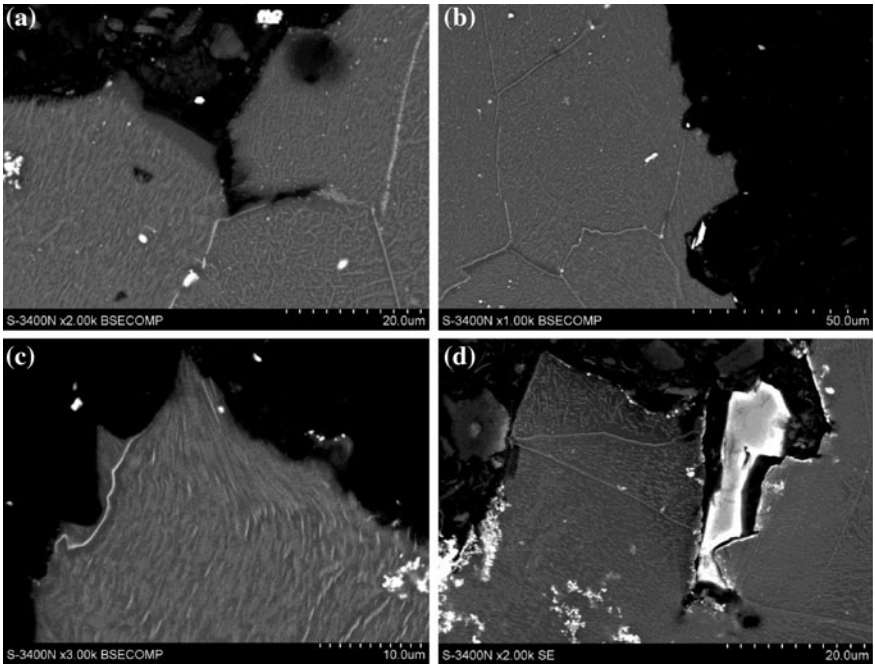

Fig. 17 Fracture surface of the crept composites, SEM; **a** cracks propagating through the denuded zones; **b** intercrystalline fracture; **c** plastic deformation at the fracture profile; **d** broken SiC/WE43 interfaces

Secondary cracks are propagating through the denuded zones at the grain boundaries (Fig. 17a). This leads to the formation of intergranular fracture. The fracture often propagates also through the softened α-Mg dendrites (Fig. 17b). Signs of plastic deformation (Fig. 17c) are observed at these places, which indicates a change from the brittle fracture at ambient temperature to the more ductile character of the fracture at the 250 °C. The SiC particles observed at the fracture surface are detached from the matrix, which indicates that fracture propagates preferentially through the SiC/WE43 interfaces (Fig. 17 c, d).

4 Discussion

The WE43 MMC reinforced with SiC particulates were prepared by means of stir casting. Investigations revealed that the application of SiC particulates with a mean diameter of 45 μm enables achieving a relatively uniform distribution of reinforcement. The addition of larger particles causes the settling down of the reinforcement both in the crucible and mould. The introduction of smaller particles led to the formation of numerous agglomerates after stirring at 720 °C. The distribution

of the small particles is relatively homogenous after stirring the melt at 780 °C. However, at this temperature, significant reactions between the reinforcement and the liquid alloy take place. The reactions lead to formation of yttrium containing phases. Formation of these phases leads to the depletion of the composite matrix in yttrium, which causes the lack of age-hardening response.

Stirring at 720 °C seems to be a relatively good compromise between the homogenous distribution of 45 μm particles and the reasonably small reaction between the liquid alloy and SiC. Literature [16] suggests the mechanism of degradation of SiC particle with molten magnesium. In the first stage of reaction, magnesium reacts with the SiO_2 layer covering SiC particulates. As a result, MgO and elemental silicon are formed. In the next stage, molten magnesium reacts with SiC, leading to its dissolution. Elemental carbon may precipitate in the form of graphite, reacting in turn with the excess of Si and form fine β-SiC crystals. In the last stage, during cooling, as the solubility of Si in magnesium decreases, Mg_2Si phases may form. However, this mechanism is true for pure magnesium reacting with SiC. In the investigated composite, the magnesium is alloyed with Zr and Y, which are more reactive than Mg, thus, changing the above mentioned mechanism. In the composite stirred at 720 °C the Zr and Si rich layer has been found to cover the SiC particles. Additionally Y_2O_3 and Zr_2Si phases have been found at the interface. The following mechanism is suggested for the dissolution of the reinforcing phase at 720 °C. In the first stage yttrium reacts with SiO_2 layer forming Y_2O_3 in reaction (1).

$$3SiO_2 + 4Y \rightarrow 2Y_2O_3 + 3Si \tag{1}$$

The formation enthalpy of this reaction at the 720 °C is equal about -518 kJ mol^{-1} of Y_2O_3 and is about four times smaller than the enthalpy of the MgO formation in the analogical reaction (-128.5 kJ mol^{-1}). This indicates that the yttrium reaction with SiO_2 is much more favourable. As the reaction (1) created zone depleted in yttrium near the SiC particle, elemental Si from this reaction may react only with Zr or Mg. As the main Zr–Si compound found within the structure of the composite is Zr_2Si, the following reaction (2) is suggested for the second stage of particle degradation:

$$2Zr + Si \rightarrow Zr_2Si \tag{2}$$

The enthalpy of this reaction is equal to about -209 kJ mol^{-1} of Zr_2Si. The reaction (2) is also more thermodynamically favourable than the similar reaction of Mg_2Si formation, with the enthalpy of which is about -69 kJ mol^{-1}. The reaction of Zr and Mg with SiC is also possible, however, their enthalpies are higher and are equal: -145 kJ mol^{-1} for formation Zr_2Si and -5.5 kJ mol^{-1} for Mg_2Si. Thin Zr–Si layers formed at the interface seems to be a quite effective barrier for the element's diffusion and further reactions. The lack of reactions significantly depleting the matrix in yttrium enables age-hardening of the composite cast at 720 °C.

Addition of SiC particles to the WE43 magnesium alloy led to the decrease of mechanical properties of the as-cast composite. The tensile strength decreased with increasing reinforcement size and its volume fraction. Yield strength, however, did not decreased significantly after the addition of SiC particles. Only in the case of the addition of large, 250 μm particles, a decrease in yield strength was observed. Similar tendencies are observed in the case of the heat treated composite reinforced with 45 μm. The tensile strength of the heat treated material decreases with increasing SiC volume fraction, while yield strength does not decrease. It can be stated that ultimate tensile strength is affected by the SiC addition, while yield strength of the composite depends only on the state of the WE43 matrix. Many authors present results of their investigations on the mechanical properties of SiC reinforced magnesium alloys. It can be stated that addition of the SiC particles may lead to an increase of material mechanical properties, which is not in agreement with our investigations. However, our research was conducted on composites reinforced with relatively big particulates, which may act as structural notches, decreasing materials' mechanical properties. On the other hand, applications of smaller SiC particulates during conventional stir casting of WE43 magnesium alloys with stirring conducted in the liquid state is difficult, due to the formation of SiC agglomerates and significant reaction between the reinforcement and liquid metal. Some research [10, 17] was done on the promising stir casting technique with stirring in the semi-solid state, slightly below the liquidus line of the alloy. Small particles may be successfully introduced to the alloy with this technique, ensuring an increase of material properties.

The creep strength of the composites is also decreasing with increasing particulates volume fraction. Cabbibo et al. [18] found that the main strengthening mechanisms at 250 °C for SiC reinforced Mg-RE alloys are, decreasingly: Hall-Petch matrix strengthening with grain and cells boundaries; Strengthening by mismatch in thermal expansion of SiC particles and the matrix; Orowan strengthening of the matrix; Load transfer between the particle and matrix and few more, less important. All these factors lead to an increase of creep resistance of the SiC strengthened WE43 alloy. However, it is again true for the particles smaller than 10 μm. The presence of big particles probably does not ensure effective strengthening by mismatch in thermal expansion coefficients. Presence of the particles detached from the matrix on the fracture surface clearly indicates that SiC/WE43 interface in the investigated composite is not strong enough to transfer the loads to the particle.

5 Conclusions

1. WE43 MMC reinforced with 45 μm SiC particulates were successfully produced by stir casting. Stirring of the melt at 720 °C leads to formation of uniform microstructure with SiC particles present at grain boundaries.

2. WE43 MMC reinforced with SiC particulates cast at 720 °C exhibit strong response to age hardening, which significantly increases mechanical properties of the composites.
3. Addition of SiC particulates causes an increase in hardness of the WE43 alloy. However it decreases the tensile strength of the material. With increasing volume fraction of the reinforcement, the tensile strength of the composite both in as-cast and heat treated condition decreases.
4. Addition of SiC particulates does not influence the yield strength of the material, the yield strength is rather dependent upon the WE43 matrix state.
5. Creep resistance of the composite decreases with increasing volume fraction of SiC reinforcement.

Acknowledgments The present work was supported by the National Centre for Research and Development under the project LIDER/29/198/L-3/11/NCBR/2012

References

1. Friedrich H, Mordike BL (2006) Magnesium technology, metallurgy, design data, applications. Springer, Berlin
2. Luo AA (2004) Recent magnesium alloy development for elevated temperature applications. Int Mater Rev 49:13–30
3. Rzychoń T, Adamczyk-Cieślak B, Kiełbus A et al (2012) The influence of hot-chamber die casting parameters on the microstructure and mechanical properties of magnesium-aluminum alloys containing alkaline elements. Mat-wiss u Werkstofftech 43:421–426
4. Dybowski B, Kiełbus A, Jarosz R (2014) Effect of mould components on the cooling rate, microstructure, and quality of We43 Magnesium casting alloy. Arch Metall Mater 59:1527–1532
5. Kiełbus A, Rzychoń T (2011) The intermetallic phases in sand casting Magnesium alloys for elevated temperature. Mater Sci Forum 690:214–217
6. Rzychoń T, Kiełbus A, Lityńska-Dobrzyńska L (2013) Microstructure, microstructural stability and mechanical properties of sand-cast Mg-4Al-4RE alloy. Mater Charact 83:21–34
7. Ferkel H, Mordike BL (2001) Magnesium strengthened by SiC nanoparticles. Mater Sci Eng A 298:193–199
8. Rashad M, Pan F, Asif M et al (2014) Powder metallurgy of Mg-1 %Al-1 %Sn alloy reinforced with low content of graphene nanoplatelets (GNPs). J Ind Eng Chem 20:4250–4255
9. Shen MJ, Wang XJ, Zhang MF et al (2014) Fabrication of bimodal size SiCp reinforced AZ31B magnesium matrix composites. Mater Sci Eng A 601:58–64
10. Wang XJ, Wang NZ, Wang LY et al (2014) Processing, microstructure and mechanical properties of micro-SiC particles reinforced magnesium matrix composites fabricated by stir casting assisted by ultrasonic treatment processing. Mater Des 57:638–645
11. Lu L, Lim CYH, Yeong WM (2004) Effect of reinforcements on strength of Mg 9 %Al composites. Compos Struct 66:41–45
12. Tzamtzis S, Barekar NS, Hari Babu N et al (2009) Processing of advanced Al/SiC particulate metal matrix composites under intensive shearing—A novel Rheo-process. Compos A 40:144–151
13. Kiełbus A, Rzychoń T (2011) Mechanical and creep properties of Mg-4Y-3RE and Mg-3Nd-1Gd magnesium alloys. Procedia Eng 10:1835–1840

14. Nie JF, Muddle BC (2000) Characterisation of strengthening precipitate phases in a Mg–Y–Nd alloy. Acta Mater 48:1691–1703
15. Mengucci P, Barucca G, Riontino G et al (2008) Structure evolution of a WE43 Mg alloy submitted to different thermal treatments. Mater Sci Eng A 479:37–44
16. Epicier T, Bosselet F, Viala JC (1994) Microstructure of interfaces between a magnesium matrix and preoxidized silicon carbide particles. Interface Sci 1:213–221
17. Aravindan S, Rao PV, Ponappa K (2015) Evaluation of physical and mechanical properties of AZ91D/SiC composites by two step stir casting process. J Magnes Alloys 3:52–62
18. Cabibbo M, Spigarelli S (2011) A TEM quantitative evaluation of strengthening in an Mg–RE alloy reinforced with SiC. Mater Charact 62:959–969